A new methodology for identifying location errors in 5-axis machine tools using a single ballbar set-up

Flynn, Joseph; Shokrani, Alborz; Vichare, Parag; Dhokia, Vimal; Newman, Stephen

Published in:
The International Journal of Advanced Manufacturing Technology

DOI:
10.1007/s00170-016-9090-6

E-pub ahead of print: 26/07/2016

Document Version
Peer reviewed version

A New Methodology for Identifying Location Errors in 5-Axis Machine Tools Using a Single Ballbar Set-up

J. M. Flynn A*[1], A. Shokrani[1], P. Vichare[2], V. Dhokia[1] and S. T. Newman[1]

[1]Department of Mechanical Engineering, University of Bath, Bath BA2 7AY, UK
[2]School of Engineering & Computing, University of the West of Scotland, Paisley PA1 2BE, UK

Received: 27 November 205 / Accepted: 23 June 2016

Abstract

Ballbar testing of rotary axes in 5-axis machine tools can be time-consuming and requires high levels of operator expertise; especially in the set-up process. Faster tests reduce down-time and encourage frequent updates to compensation parameters to reflect the current state of the machine. A virtual machine tool (VMT) is developed to emulate the machine tool, its geometric errors and the testing procedures. This was used to develop a new single set-up testing method to identify all rotary axis locations errors, whilst remaining robust in the presence of set-up error and linear axis squareness errors. New testing and data processing techniques remove the requirement for fine adjustment of the tool-cup and permit full automation of necessary toolpaths, including transitions. Using the VMT, error identification residuals were found to be 2.7% or less. Experiments and statistical analysis then showed that all errors can be measured using a single set-up, and values are sufficiently close to the values measured using conventional multi-set-up procedures to be used in error compensation. This method will significantly reduce set-up durations and removes the need for any modified testing hardware.

Keywords: Ballbar, Five-Axis Machine Tool, Error

1 Introduction

Five-axis machine tools can manufacture complex three-dimensional parts, with sculptured surfaces and overhanging features; often using fewer set-ups than three-axis alternatives. To increase the in-service performance of machined components and to accommodate automated assembly processes, part complexity is increasing and dimensional tolerances are becoming ever-tighter [1]. Hence, academic and industrial research has focused on the development of instrumentation and processes to support measurement and compensation of errors in machine tool axes [2, 3].

Conceived by Bryan in 1982 [4], the Telescoping Magnetic Ballbar (TMBB) has been widely adopted in the verification of three-axis machine tool errors. Its repertoire is now being extended to include the verification of rotary axes in multi-axis machines. ISO 230-1:2012 [5] and ISO 10791-6:2014 [6] now both specify the TMBB as a method to verify geometric errors in rotary axes, which is testament to the significant quantity of research undertaken in this area. This paper aims to identify rotary axis location errors in a five-axis machine tool, whilst remaining robust in the presence of linear axis squareness errors and apparatus set-up errors. It aims to achieve this using a single testing set-up, without the need for manual adjustments to remove set-up errors, and without employing kinematic model-based optimization to fit geometric error values to TMBB length measurements.

*j.m.flynn@bath.ac.uk

1.1 State-of-the-art Five-Axis TMBB testing methods

Kakino et al. [7] and Sakamoto and Inaskai [8] identified the importance of strategically aligning TMBB to increase sensitivity to specific geometric error sources in rotary axis testing. In general, the TMBB may be aligned to either a Cartesian or cylindrical coordinate system frame of reference. Cartesian alignments include the X, Y or Z-directions, whereas cylindrical alignment is typically radial, axial or tangential with respect to the rotary axis average line [5, 6, 9]. The use of a cylindrical coordinate system was popularised by the 2003 work of Tsutsumi and Saito [9], who identified that radial offset errors and tilt errors could be identified by relating the eccentricity of the least squares circles, fitted to the TMBB measurements. Later, in 2013, Tsutsumi et al. [10] made a formal comparison of cylindrical and Cartesian TMBB alignments. It was concluded that both methods were effective, but the cylindrical alignment was less susceptible to corruption in the presence of set-up errors, adding robustness to the analysis.

Cartesian TMBB are still widely used due to their ability to identify both location and component errors in rotary axes [11–14], which is generally not possible (or very difficult) with cylindrically aligned tests. This is because cylindrically aligned tests identify errors by fitting functions to all measurements in a toolpath, whereas Cartesian aligned tests can consider individual measurements. Interestingly, most, if not all, existing methods for identifying component errors in rotary axes require the centre-pivot to be coincident with the rotary axis average line, which is not always possible [11–14].

When a cylindrical TMBB alignment is employed, radial offset errors of rotary axes are identified using a radially aligned TMBB tests (e.g. [9]). Conversely, there are two prevailing methods for identifying the orientation errors of a rotary axis. The first method uses an axially aligned TMBB to identify the tilt errors directly (e.g. [9]). Alternatively, radially aligned TMBB tests may be conducted at two axially separated locations to identify the centre of rotation at two points. The rotary axis average line is characterised by the vector between these two centres, which may be queried to identify the orientation errors e.g. [11, 15, 16].

Recently, oblique-radial testing methods [17–20, 13] have gained in popularity. They utilise a conventional radial test in conjunction with a second test that is part-way between an axially and radially aligned test. This is advantageous in the sense that radial offset and orientation errors may be identified whilst the tool-cup remains stationary on the rotary axis average line. This removes the need for synchronised interpolations between the linear and rotary axes to maintain the TMBB alignment. Potential drawbacks of these methods include the need to install an extension bar to increase the TMBB length for the oblique tests, and the added complexity of having radial offset error effects present in both radial and oblique radial tests.

Finally, several studies have explored the use of arbitrary TMBB tool-paths to identify errors, focussing on acquiring measurement data from a large number of distributed machine poses. Rather than fitting a geometry (or any function of a specific form) to the measurement data, the kinematic model of the machine tool is used to identify a combination of error values that minimises the residual between predicted and measured TMBB lengths. Model fitting via the formation of identification Jacobian matrices has been used to calculate location errors in both linear and rotary axes [21, 22]. Although these methods provide a powerful error identification tool, their standardisation is challenging due to the lack of specificity in their tool-paths and set-ups. Additionally, the need for a detailed kinematic model of the machine tool, combined with the mathematical complexity of the error identification procedures make this an expert technique.

1.2 Limitations and assumptions in existing TMBB testing methods

Much of the research that addresses the identification of geometric errors in rotary axes utilise broad assumptions that may limit the usefulness of the measurement data in an operational scenario. Firstly, there is often an assumption that no errors (component or location) exist in the linear axes [9, 10, 20]. Only four publication address this issue by including linear axis location errors in the identification process. Li et al. [23] included linear axis squareness effects in their identification of rotary axis location

errors, and Tsutsumi et al. [24] conducted similar research in conjunction with a non-orthogonal rotary axis configuration. Likewise, [21, 22] both incorporate linear axis squareness in their model-based optimisation of error parameters. This area of research is comparatively under-explored when considering rotary axis location errors. Until such a time that these errors are readily included in rotary axis tests, measurement outcomes will be limited by the need to pre-calibrate linear axis errors, which is a time-consuming process.

Other existing methods are only suited to specific machine tool configurations, as the tool-tip must be placed on the average line of the rotary axis under scrutiny [25]. This is rarely possible in small-to-medium-sized machine tools with tilting-rotary tables and machines with two rotary axes in an articulating head. This is closely related to the above issue, as synchronised interpolation between linear and rotary axes is necessary, subjecting measurements to corruption by linear axis errors.

Testing two rotary axes generally requires at least two unique testing set-ups, which increases testing durations and the number of unique set-up errors in testing data. If error values are identified using previously measured parameters, it becomes necessary to measure the set-up errors such that results from each set-up can be mapped onto each other. This has been considered in [26, 21, 22]. In [26], a synchronised four-axis interpolation (Y, Z, A and C) is used with a single set-up; however, not all errors can be identified correctly using this method, without the use of a second set-up. The works of [21, 22] use arbitrary tool-paths, a model-based optimisation of errors and single set-up. The work of [21] has not been experimentally validated, despite promising simulation results, whereas [22] has demonstrated successful implementation on a machine tool. The need for complex kinematic models to facilitate error identification makes it cumbersome to verify multiple machines. Their standardisation is also challenging due to their lack of specificity in the testing set-up and tool-paths.

Some earlier research gave no provision for dealing with tool-tip or centre-pivot set-up errors (e.g. [9, 20]). Research is now addressing this issue by specifying techniques to manually remove tool-cup errors through the use of a modified, adjustable tool-cup e.g. [16] and ISO 10791-6:2014 [6]. Sensitivity analysis has been undertaken to identify the severity of the effects of set-up errors on TMBB trajectories [11, 13, 16]. In each case, one-factor-at-a-time (OFAT) sensitivity analysis has been used to characterise individual effects. Methods incorporating arbitrary tool-paths with a model-based optimisation of error parameters have included tool-cup and centre-pivot errors in this process, treating them as variables to be identified [21, 22]. The work of [22] comments on the fact that set-up errors are confounded with axis geometric errors, but choose to attribute as much error as possible to the testing set-up. In contrast, this confoundedness is not commented upon in [21].

1.3 Issues addressed in this research

This research addresses the issues identified in the previous section through the development of a single set-up testing procedure that can be fully automated. This procedure only uses toolpaths that are found in ISO 230-1:2012 [5] and ISO 10791-6:2014 [6] so that it may be standardised across various machine tool configurations, whilst retaining the ability to easily program the toolpaths in the NC control. Once captured, the measurement data is processed using a combination of algorithms that are not heavily reliant on a complex kinematic model. These algorithms have the ability to separate the effects of linear and rotary axis location errors, increasing the robustness of the procedure under operational conditions (i.e. imperfect linear axes). Finally, the method is also robust in the presence of set-up errors in both tool-cup and centre-pivot, furthering the usefulness of the measured error values. The outcome of this research is a testing procedure that permits end-users to rapidly verify machine tool geometric accuracy, with improved confidence in the measured result. This supports go, no-go decisions regarding the machines readiness to perform manufacturing tasks, and also to informs subsequent machine tool compensation activities.

In this paper, the principle of the single set-up testing method is described, proving its efficacy through the use of a virtual machine tool (VMT) developed as part of this research (Section 2.3). A method for separating linear and rotary axis location errors is described and shown to be effective using the VMT (Section 2.5 and 2.6). Finally, a OFAT sensitivity analysis is conducted to identify the effects

Table 1: Machine tool location errors for both linear and rotary axes, as defined in ISO 230-1:2012

Notation	Error Definition
E_{C0X}	Squareness of X to Y
E_{A0Z}	Squareness of Z to Y
E_{B0Z}	Squareness of Z to X
E_{X0B}	Y-offset from B to C
E_{A0B}	Parallelism error of B to Y in the reference YZ-plane
E_{C0B}	Parallelism error of B to Y in the reference XY-plane
E_{A0C}	Squareness of C to Y
E_{B0C}	Squareness of C to X

of set-up errors on each testing tool-path (Section 2.8). This is then used to inform the development of an automated compensation scheme for these effects, which does not require an adjustable tool-cup. For each of the investigations, above, experiments are conducted on a commercial 5-axis machine tool to analyse their advantages and limitations. Rigorous statistical analysis is undertaken on repeated measurements to give a commentary on the success of the proposed methodology (Sections 3 and 4).

2 Methodology

The design of a new 5-axis machine tool TMBB ballbar testing method requires significant verification to ensure its validity. Therefore, this research presents a two-fold validation of all aspects of the testing method; simulation in a VMT and experimental validation on a commercial 5-axis machine tool. The development of the VMT is discussed, results from simulations presented and experimental procedures outlined.

2.1 Machine tool kinematic configuration

The kinematic modelling, simulation and experiments of this research have been conducted using an XYZ 1020 VMC 5-axis machine tool. A schematic of this machine is given in Figure 1. In accordance with the axis nomenclature specified in ISO 841:2001 [27], the kinematic configuration is denoted [wC'B'X'Y'bZ(C)t]. This may be read as workpiece, C-axis, B-Axis, X-axis, Y-axis, machine tool base, Z-axis, machine tool spindle, and tool-tip. Here, the axes are given by their traditional Cartesian designation, with the C-axis rotating about the Z-direction and the B-axis rotating about the Y-direction. Close attention should be paid to the inclusion of the (') notation, which represents an axis contained in the kinematic chain spanning between the foundation and the workpiece. This signifies that the axis is actuated in the opposite direction to create the correct relative movement between the tool and the workpiece coordinate system during NC programming.

As described in Annex A of ISO 230-1:2012 [5] and further explained in [3], a minimal set of eight error parameters are required to characterize the controlled axes of a 5-axis machine tool. There are a further four error parameters associated with the spindle; however, these have not been included in the analysis throughout this research. The eight error parameters are defined using the definitions and notations given in Table 1. These eight error parameters require the appropriate assignation of the machine tool coordinate system origin in order to be sufficient. The origin of the coordinate system is placed along the C-axis average line, located the same Z-height as the point at which the B-axis intersects the ZX-plane. This location is indicated in Figure 1. As the Y-axis is closest to the machine tool foundation it may be intuitively taken as the datum axis, and all errors defined in Table 1 have been defined with this in mind.

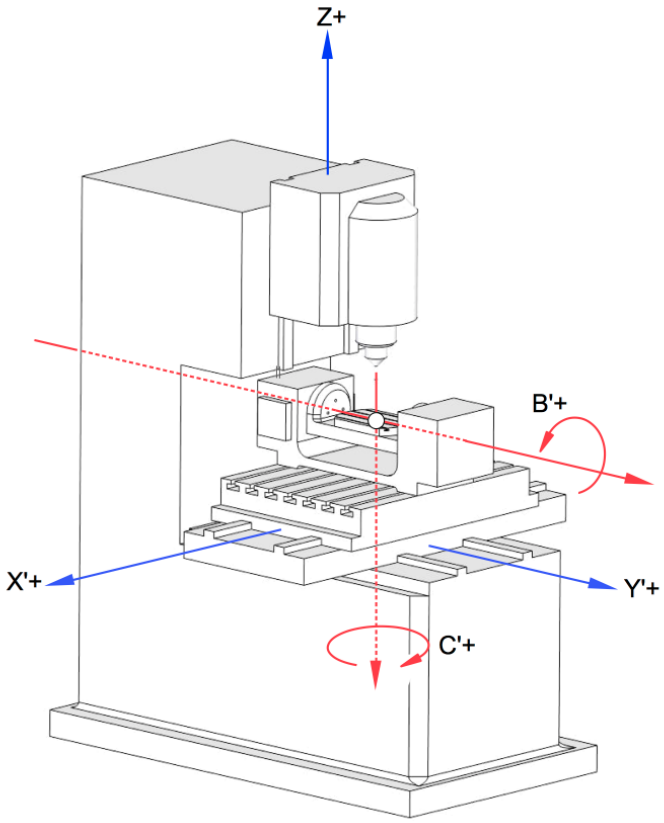

Figure 1: Schematic of the axis configuration found on the XYZ 1020 VMC machine tool used for the experiments in this research

2.2 Kinematic modelling of a 5-axis machine tool and its location errors

The majority of the methods detailed Sections 1.1 and 1.2 use sequential multiplication of homogeneous transformation matrices to model machine tool kinematics. Considering location errors only, the general formulation of a linear axis transformation matrix, with respect to the frame upon which it is mounted consists of the multiplication of two matrices: ${}^{Y'}_{b'}\mathbf{T}_{\mathbf{pos}}$ describes the nominal position and orientation of the axis, ${}^{Y'}_{b'}\mathbf{T}_{\mathbf{loc}}$ describes the location errors of the axis.

$$ {}^{Y'}_{b'}\mathbf{T}_{\mathbf{pos}} = \begin{bmatrix} -1 & 0 & 0 & X_{0Y} \\ 0 & -1 & 0 & Y_{0Y} \\ 0 & 0 & 1 & Z_{0Y} \\ 0 & 0 & 0 & 1 \end{bmatrix}, \qquad {}^{Y'}_{b'}\mathbf{T}_{\mathbf{loc}} = \begin{bmatrix} 1 & 0 & 0 & -y \cdot E_{C0Y} \\ 0 & 1 & 0 & y \\ 0 & 0 & 1 & y \cdot E_{A0Y} \\ 0 & 0 & 0 & 1 \end{bmatrix} $$

Here, the '·' notation represents multiplication. A rotary axis is similarly represented: ${}^{B'}_{X'}\mathbf{T}_{\mathbf{pos}}$ describes the nominal position and orientation, ${}^{B'}_{X'}\mathbf{T}_{\mathbf{loc}}$ describes the location errors of the axis, and ${}^{Y'}_{b'}\mathbf{T}_{\mathbf{rot}}$ describes the actuation of the axis.

$$ {}^{B'}_{X'}\mathbf{T}_{\mathbf{pos}} = \begin{bmatrix} 1 & -C_{0B} & 0 & X_{0B} \\ C_{0B} & 1 & -A_{0B} & Y_{0B} \\ 0 & A_{0B} & 1 & Z_{0B} \\ 0 & 0 & 0 & 1 \end{bmatrix}, \qquad {}^{B'}_{X'}\mathbf{T}_{\mathbf{loc}} = \begin{bmatrix} 1 & -E_{C0B} & 0 & E_{X0B} \\ E_{C0B} & 1 & -E_{A0B} & 0 \\ 0 & E_{A0B} & 1 & E_{Z0B} \\ 0 & 0 & 0 & 1 \end{bmatrix} $$

$$
{}^{B'}_{X'}\mathbf{T}_{\mathbf{rot}} = \begin{bmatrix} \cos(B) & 0 & \sin(B) & 0 \\ 0 & 1 & 0 & 0 \\ -\sin(B) & 0 & \cos(B) & 0 \\ 0 & 0 & 0 & 1 \end{bmatrix}
$$

The general axis transformation is given in (1) and is denoted ${}^{i}_{i-1}\mathbf{T}$:

$$
{}^{i}_{i-1}\mathbf{T} = \begin{cases} {}^{i}_{i-1}\mathbf{T}_{\mathbf{pos}_{i-1}}{}^{i}\mathbf{T}_{\mathbf{loc}}, & \text{linear} \\ {}^{i}_{i-1}\mathbf{T}_{\mathbf{pos}_{i-1}}{}^{i}\mathbf{T}_{\mathbf{loc}_{i-1}}{}^{i}\mathbf{T}_{\mathbf{rot}}, & \text{rotary} \end{cases} \tag{1}
$$

To express the j^{th} element of a kinematic chain with respect to the base frame (zeroth frame), the multiplication in (2) is required.

$$
{}^{j}_{0}\mathbf{T} = \prod_{i=1}^{j} {}^{i}_{i-1}\mathbf{T} \tag{2}
$$

By completing this transformation for all kinematic chains in the machine tool, the extremities (e.g. workpiece and tool-tip) can be expressed with respect to the common machine tool coordinate system, which helps to identify position and orientation errors between the tool-tip and workpiece.

2.3 A virtual environment for kinematic modelling and machine simulation

The use of homogeneous transformation is widespread in machine tool modelling; however, if a different machine tool is considered, these matrices would need to be redefined, which is undesirable. Taking inspiration from the work of Fesperman et al. [28], a VMT has been developed in the MATLAB R2014b software package [29]. The user can define and interchange new machine tools, testing tool-paths and error source profiles to simulate different machine tool metrology scenarios (Figure 2). This model differs from the work of [28] insomuch as it focuses more on sensitivity analysis and tool-path design. The general user interaction with the VMT is described using an IDEF0 diagram as shown in Figure 3.

Location and set-up error sources are defined using either a specific value (e,.g. zero) or a randomly generated value between an upper and lower limit. Using the forward kinematics module, the position and orientation of each axis frame is identified to calculate the length of the TMBB and also to place geometrical primitives in a machine tool animation. Testing tool-paths are described in the testing set-up pop-up window. Here, only axial and radial tests have been defined; however, any tool-path can feasibly be modelled.

2.4 Measurement procedure using a single testing set-up

The proposed single set-up testing method uses a single, off-axis centre pivot position, which is described by the parameters O_x, O_y, and O_z. These offsets are measured with respect to the machine tool coordinate system as per the definition given earlier in this paper. Additionally, the nominal TMBB length is denoted, L_0. These parameters are described visually in Figure 4. This set-up is akin to the C-axis testing set-up used in [9]. Four unique tool-paths are conducted using this set-up: Radial B, Axial B, Radial C and Axial C, as prescribed by ISO 10791-6:2014 [6]. These are shown schematically in Figure 5, and the testing parameters used in the experiments throughout this research are given in Table 2. Transitions between tests are easily programmed using conventional circular interpolations to relocate the tool-cup.

In this research, an axis of rotation is modelled as a unit vector attached to a point in space. The unit vector describes the orientation of the axis and the point in space represents the location of the rotary axis average in some coordinate frame of reference. Assuming that the machine tool may be modelled using rigid body motion and that only location errors act in the system, it can be said that a rotary axis may be characterised with equal validity at any point along the average line.

The error identification algorithms outlined as part of this research may be broken down into two sub-problems: (i) The centroid of the least-squares circle applied to radially-aligned test data is analogous

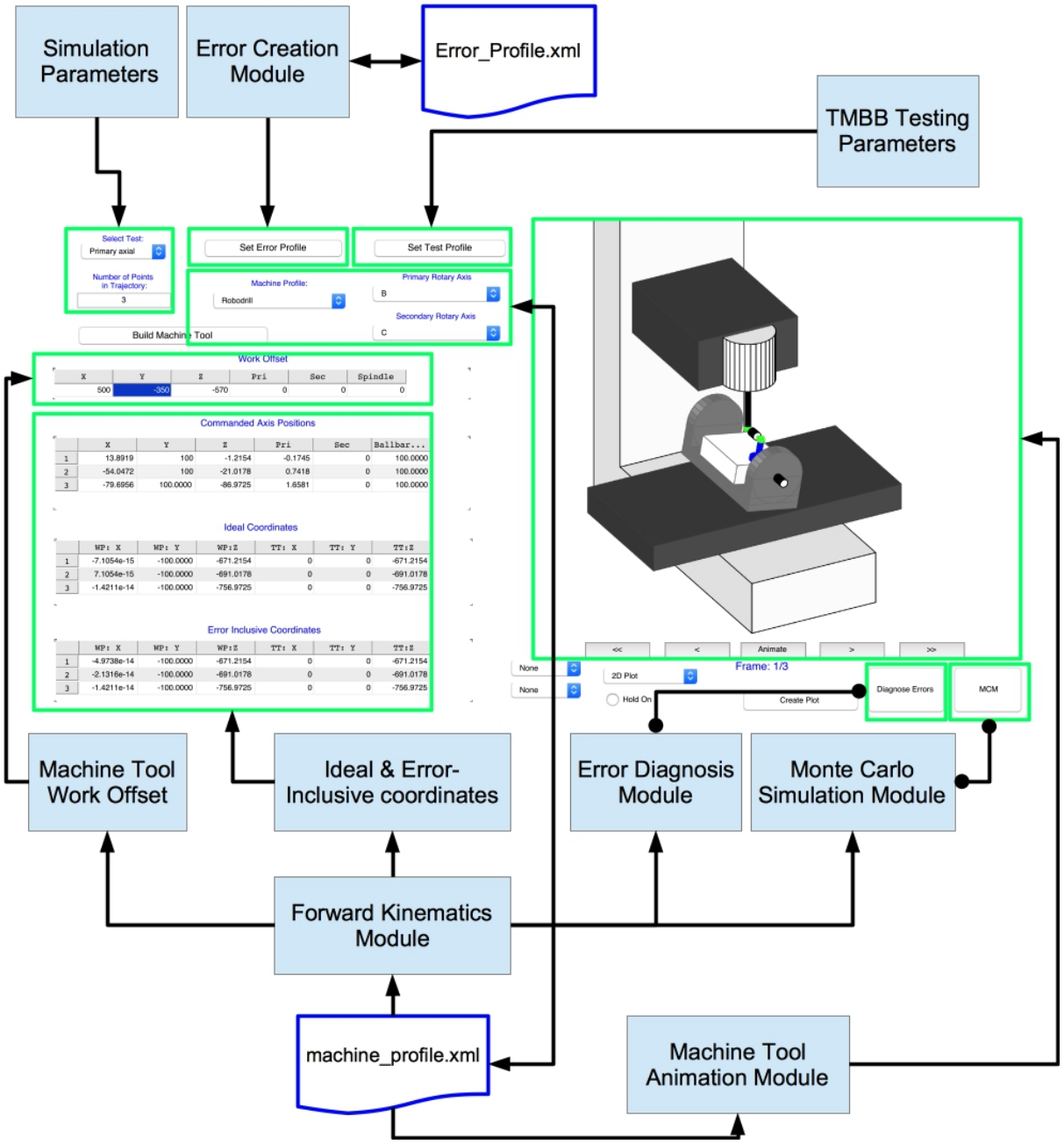

Figure 2: Graphical user interface for virtual machine tool model

Table 2: Set-up and testing parameters used in virtual and empirical validation of the methods outlined in this research

	Centre-Pivot Offsets [mm]			Tool-Cup Offsets [mm]			Angle of Arc [°]		
Test	O_x	O_y	O_z	TC_x	TC_y	TC_z	θ_{start}	θ_{end}	L_0
Radial B	0	−85	159.982	0	−85	259.892	−10	95	100
Axial B	0	−85	159.982	0	15	159.892	−10	95	100
Radial C	0	−85	159.982	0	15	159.892	−10	95	100
Axial C	0	−85	159.982	0	−85	259.892	−10	95	100

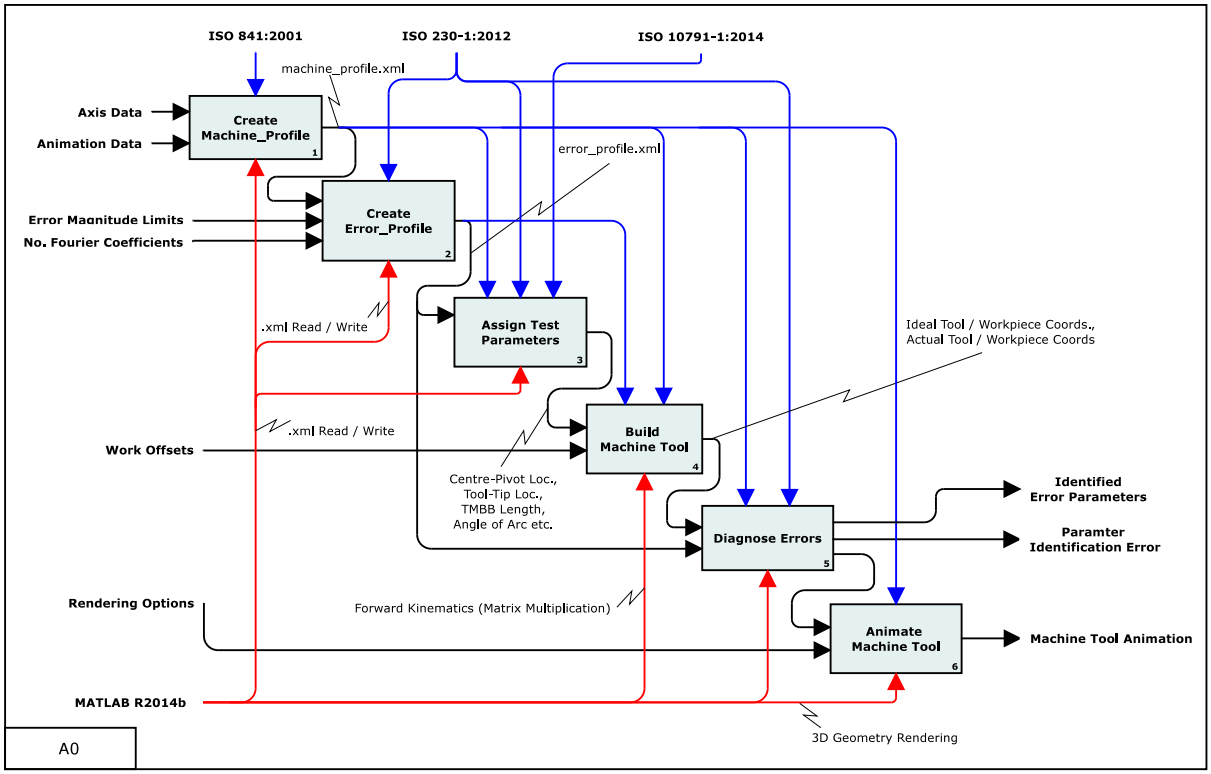

Figure 3: IDEF0 diagram of virtual machine tool modelling process

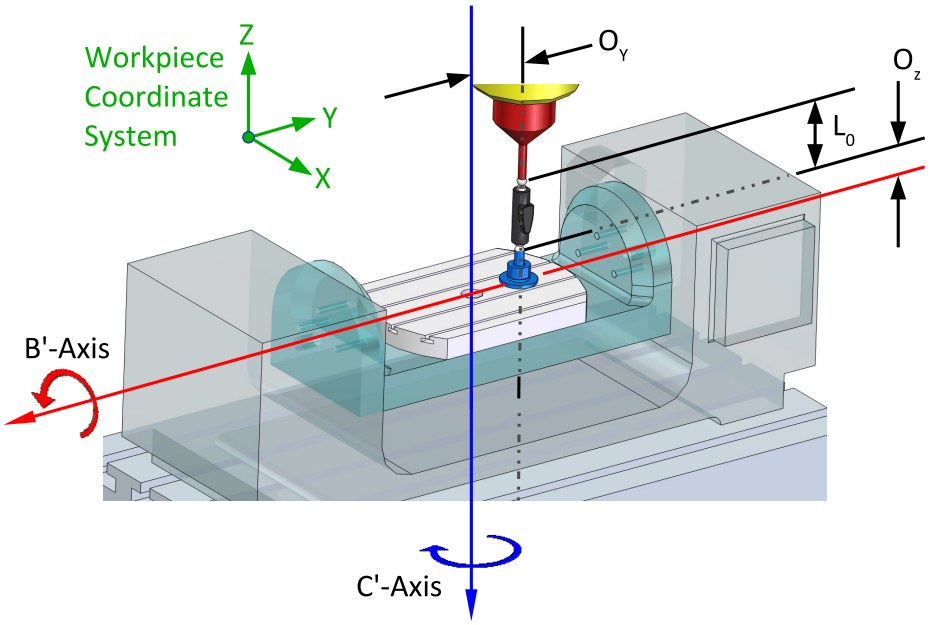

Figure 4: A description of the single testing set-up

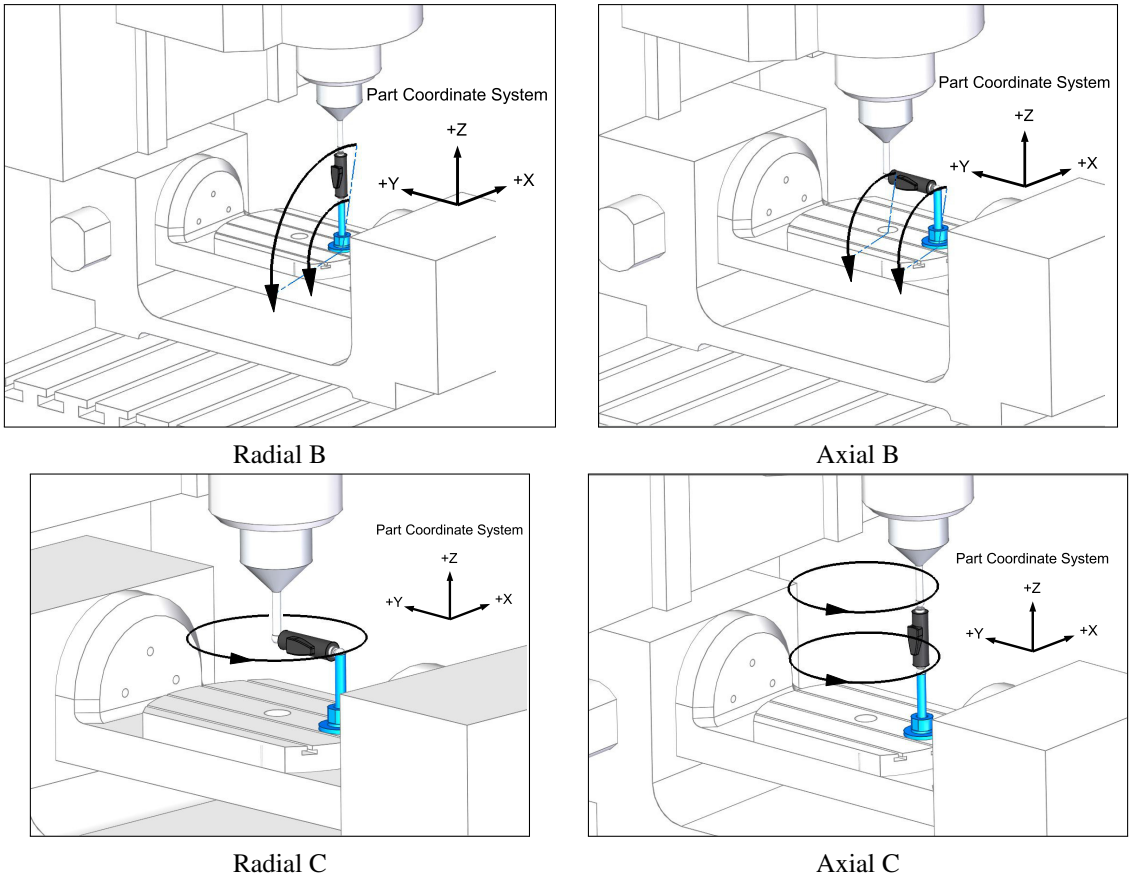

Figure 5: Four tool-paths used to verify the location errors of the primary and secondary rotary axes

to the radial coordinates of a point along the rotary axis average line. (ii) The least squares plane fitted to the axially-aligned test data identifies the normal vector of a plane that is parallel to the plane of rotation and the axial coordinate of the point along the average line. For the B-axis, the centroid of the least-squares circle is denoted (C_x, C_z) and for the C-axis (C_x, C_y) is used. The unit vectors components from the plane fits are denoted $[U_x, U_y, U_z]$. It is assumed that three planar linear axis TMBB tests are sufficient to accurately measure the linear axis squareness errors in support of the proposed rotary axis testing and data-processing methods.

2.5 Identifying the radial coordinates of a point on the rotary axis average line

For radially aligned tests, a least-squares circle is fitted to the perceived centre-pivot coordinates. The fitting procedure is in accordance with the hyper-fit algorithm detailed in [30], which has been chosen for its zero essential bias. The centre-pivot coordinates are approximated using the perceived tool-tip coordinates and the measured TMBB length. In the presence of linear axis squareness errors, it is known that a circular planar motion described by two nominally orthogonal linear axes adopts an elliptical appearance. The semi-major axis of the ellipse will be aligned to either the $\pm 45^\circ$ position between the two axes. Taking the Y-axis as the datum axis, there is one squareness error in X relative to Y, and two squareness errors in Z, relative to X and Y; creating an oblique coordinate system. Using small angle approximations and omitting higher order terms, motion within this coordinate system is described with the transformation matrix in (3).

$$\begin{bmatrix} x_{actual} \\ y_{actual} \\ z_{actual} \end{bmatrix} = \begin{bmatrix} 1 & 0 & E_{B0Z} \\ E_{C0X} & 1 & -E_{A0Z} \\ 0 & 0 & 1 \end{bmatrix} \begin{bmatrix} x_{ideal} \\ y_{ideal} \\ z_{ideal} \end{bmatrix} \tag{3}$$

To solve the problem of identifying the radial coordinates of a point along the rotary axis average line, the perceived tool-tip coordinates are required. During the Radial B-axis test, tool-tip coordinates are expressed using (3), with ideal coordinates $[x_{ideal}, y_{ideal}, z_{ideal}]^T$ calculated using (4):

$$\begin{bmatrix} x_{ideal} \\ y_{ideal} \\ z_{ideal} \end{bmatrix} = \begin{bmatrix} \cos(B) & 0 & sin(B) \\ 0 & 1 & 0 \\ -\sin(B) & 0 & \cos(B) \end{bmatrix} \begin{bmatrix} O_x \\ O_y \\ O_z + L_0 \end{bmatrix} \tag{4}$$

Using the actual tool-tip coordinates from (4), a unit vector describing the approximate orientation of the TMBB's sensitive direction is constructed. This unit vector describes the direction of the TMBB, connected between the 'actual' tool-tip coordinates and the nominal centre-pivot coordinates. The nominal coordinates of the centre-pivot are calculated using (5):

$$\begin{bmatrix} x_{CP} \\ y_{CP} \\ z_{CP} \end{bmatrix} = \begin{bmatrix} \cos(B) & 0 & sin(B) \\ 0 & 1 & 0 \\ -\sin(B) & 0 & \cos(B) \end{bmatrix} \begin{bmatrix} O_x \\ O_y \\ O_z \end{bmatrix} \tag{5}$$

The approximate TMBB vector is therefore:

$$\mathbf{v_{BB}} = \begin{bmatrix} x_{CP} - x_{actual} \\ y_{CP} - y_{actual} \\ z_{CP} - z_{actual} \end{bmatrix} \tag{6}$$

$$\mathbf{u_{BB}} = \frac{\mathbf{v_{BB}}}{\|\mathbf{v_{BB}}\|} \tag{7}$$

The measurement data is integrated within the model, and the approximation of the centre-pivot location, $\mathbf{p_{CP}}$, is calculated using the actual tool-tip location, $\mathbf{p_{TT}}$, the direction unit vector of the TMBB, $\mathbf{u_{BB}}$, and the measured length of the TMBB, l_{BB}. It is the coordinates of $\mathbf{p_{CP}}$ that are used in the least-squares circle-fitting algorithm and these are calculated using (8).

$$\mathbf{p_{CP}} = \mathbf{p_{TT}} - \mathbf{u_{BB}} l_{BB} \tag{8}$$

2.6 Identifying the plane of rotation and the axial coordinate of the point on the rotary axis average line

An axially aligned test measures the separation between the tool-tip and the centre-pivot in the axial direction of the rotary axis. Changes in TMBB length imply a tilt in relative motion of the centre-pivot with respect to the tool-tip. The orientation plane describing this motion is jointly affected by the linear axis squareness errors and the orientation of the rotary axis average line. If the errors introduced by the linear axes are known, they can be separated, allowing the orientation of the rotary axis to be identified using the TMBB length measurements.

Taking the B-axis as an example, the actual tool-tip motion is calculated using (3). This linear axis squareness contributes to the perceived orientation of the centre-pivot motion, relative to the tool-tip. The nominal centre-pivot motion is identified by rotating the starting position of the centre-pivot by the required B-axis angle about the nominal average line:

$$\begin{bmatrix} x_{CP} \\ y_{CP} \\ z_{CP} \end{bmatrix} = \begin{bmatrix} \cos(B) & 0 & \sin(B) \\ 0 & 1 & 0 \\ -\sin(B) & 0 & \cos(B) \end{bmatrix} \begin{bmatrix} x_{CP(start)} \\ y_{CP(start)} \\ z_{CP(start)} \end{bmatrix} \tag{9}$$

The TMBB vector for each measurement position is then defined as below, and the corresponding unit vector is calculated using (7):

$$\mathbf{v_{BB}} = \begin{bmatrix} x_{CP} - x_{TT} \\ y_{CP} - y_{TT} \\ z_{CP} - z_{TT} \end{bmatrix} \tag{10}$$

Using the TMBB measurement data and (8), the perceived centre-pivot locations were calculated. A least squares plane is fitted to these 3D centre-pivot coordinates by minimising the orthogonal distance from each coordinate to the plane. The National Institute of Standards and Technology (NIST) propose a stable algorithm [31] to conduct this fitting by taking the Singular Value Decomposition (SVD) of the matrix **A**. This matrix contains column vectors with m-rows of X, Y and Z centre-pivot coordinates. These are normalised by removing the centroid of the data, $[\bar{x}, \bar{y}, \bar{z}]$, from each point.

$$\mathbf{A} = \begin{bmatrix} x_1 - \bar{x} & y_1 - \bar{y} & z_1 - \bar{z} \\ \vdots & \vdots & \vdots \\ x_m - \bar{x} & y_m - \bar{y} & z_m - \bar{z} \end{bmatrix} = \mathbf{USV}^T \tag{11}$$

Here, **U** and **V** are orthogonal matrices, and **S** is a diagonal matrix containing the singular values. The columns of **V** are the orthonormal basis of the data. The column of **V** that corresponds to the column of the smallest singular value in **S** yields the unit vector of the least squares plane of best fit via a minimization of the orthogonal distance of the approximate centre-pivot positions to the plane. With linear axis error effects removed, this unit vector is a representation of the rotary axis orientation in the machine tool coordinate system.

The axial coordinate of the point along the rotary axis average line is calculated by evaluating the equation of the least squares plane using the radial coordinates of the point on the average line. Expressing the equation of a plane as:

$$ax + by + cz + d = 0 \tag{12}$$

The value of d is calculated by taking the dot product of the centroid of the centre-pivot position data and the unit vector, $\hat{\mathbf{u}}_\mathbf{1}$, of the rotary axis average line. The components of the unit vector correspond to a, b and c:

$$d = [\bar{x}, \bar{y}, \bar{z}] \cdot \hat{\mathbf{u}}_\mathbf{1} \tag{13}$$

In the case of the B-axis, this plane equation can be rearranged to identify the Y-coordinate of the point along the axis average line:

$$y = \frac{-d - ax - cz}{b} \tag{14}$$

This completes the characterisation of the rotary axis average line as a unit vector anchored to a point in space.

2.7 Expressing the identified axis parameters at the machine tool origin

Given that the machine tool origin is positioned at the nominal point of intersection between the primary and secondary rotary axes, shown in Figure 6 as $\mathbf{P_{1A}}$, the associated location error values should be expressed in relation to this point. Figure 6 demonstrates that a radial test conducted at the same axial location as $\mathbf{P_{1A}}$ is not affected by the tilt errors of the rotary axis as the proximity of the testing location to the machine tool origin ($\mathbf{P_{1A}}$) makes the contribution of tilt-errors negligible. If the same axis was measured at a different axial location, say, $\mathbf{P_{2A}}$, the presence of tilt and offset errors results in two mechanisms by which the point $\mathbf{P_{2C}}$ is affected. In order to express these errors in relation to the origin,

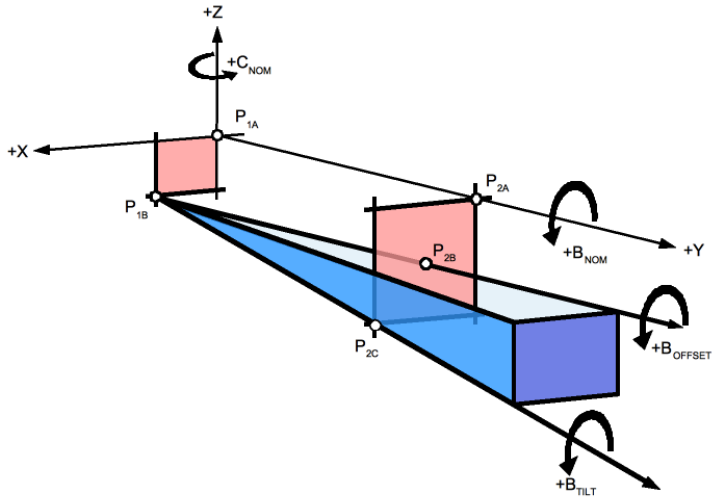

Figure 6: Illustration of the added complexity introduced by testing the B-axis with an offset centre-pivot location

the orientation of the axis average line must be known so that the point $\mathbf{P_{2C}}$ can be transported back towards the origin, yielding the offset errors observed at $\mathbf{P_{1B}}$.

To transport the rotary axis measurement parameters back to the machine tool origin, the point on the rotary axis average line is projected along the associated unit vector to the $Y = 0mm$ position. This is equivalent to finding the point of intersection between rotary axis average line and the nominal ZX-plane. Let $\mathbf{p_0}$ be a point on the nominal ZX-plane, $\mathbf{p_1}$ the point on the rotary axis average line, $\hat{\mathbf{u}}_\mathbf{0}$ is the normal vector to the ZX-plane and $\hat{\mathbf{u}}_\mathbf{1}$ is the direction unit vector of the rotary axis average line. The scalar parameter, k, denoting the distance to transport the point back to the ZX-plane is calculated using using (15). This is then used in conjunction with the vector-notation expression of the rotary axis average line to find the point of intersection, $\mathbf{p_{intersect}}$, using (16).

$$k = \frac{(\mathbf{p_0} - \mathbf{p_1}) \cdot \hat{\mathbf{u}}_\mathbf{0}}{\hat{\mathbf{u}}_\mathbf{1} \cdot \hat{\mathbf{u}}_\mathbf{0}} \tag{15}$$

$$\mathbf{p_{intersect}} = \mathbf{p_1} + k\hat{\mathbf{u}}_\mathbf{1} \tag{16}$$

2.8 Suppression and compensation of set-up errors

The previous works of [11, 16] have discussed the detrimental effects of errors in the tool-cup and centre-pivot on rotary axis ballbar tests. Tool-cup positional errors refer to offsets in the X, Y and Z-directions of the centre of the spindle mounted TMBB sphere. These are subdivided into radial and axial tool-cup errors i.e. errors in X and Y are radial and errors in Z are axial for a vertical machining centre. These errors arise from defects in the tool-cup itself, misalignment of the tool-cup within the collet or poor engagement between the shank of the tool-holder and the spindle's taper. Axial errors typically arise from an incorrectly measured tool-cup length, which is a prevailing challenge in rotary axis testing using TMBB and other metrology technologies [28].

In particular, axial tool-cup errors present a considerable challenge in rotary axis testing as this error is coupled with the offset of a horizontal rotary axis in the Z-direction (e.g. E_{Z0B}). In lieu of a method to separate these errors, existing research has specified the need to measure the tool-cup length as accurately as possible. Generally, this may be achieved using tool-setting probes that are installed on the machine tool, or through the use of a dial gauge and known-length tool (KLT). In this research, the dial gauge method is used.

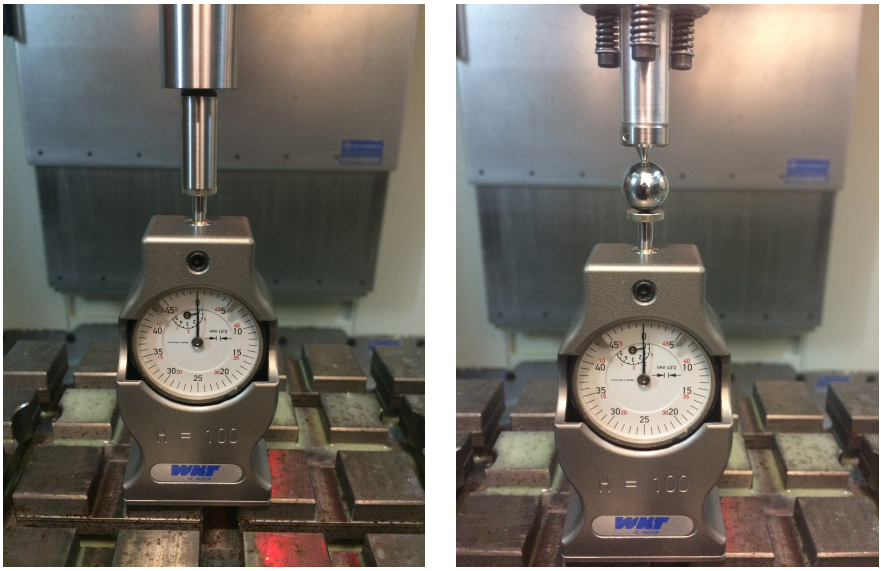

Figure 7: Photographs of the known-length tool (left) and tool-cup (right) being lowered onto the dial gauge to measure tool-cup length

The KLT is lowered onto dial gauge until the dial reads a pre-defined displacement from its free position. Once this displacement is achieved, the Z-coordinate of the datum line of the spindle in the machine tool's coordinate system is registered. Without moving the dial gauge, the tool-cup is then inserted into the spindle and is then lowered onto the dial gauge until the same predefined displacement is achieved. Once again, the Z-coordinate of the spindle's datum line is registered (Figure 7). The difference between the two registered gauge line Z-coordinates gives the difference in length between the KLT and unknown length of the tool-cup. Hence, the length of tool-cup is identified using (17). The radius of the sphere must be subtracted from this value.

$$L_{TC} = L_{KLT} - (Z_{KLT} - Z_{TC}) \tag{17}$$

In the existing literature, radial tool-cup errors have been manually removed to suppress their effects on rotary axis tests [16]. This is typically achieved with an adjustable tool-cup, used to realign the centre of the spindle mounted sphere with the spindle average line. This method is also recommended as part of the machine specific standard ISO 10791-6:2014 [6], where a device with four adjustment screws is described for realignment of the tool-cup.

It is the experience of the authors that this alignment process is time-consuming and requires moderate levels of operator skill and dexterity, which is undesirable. A preferable scenario would be to accept the presence of these errors and suppress them through processing of the TMBB length data. With this in mind, the spindle-indexing method has been conceived as a method for eliminating the need to pre-align the tool-cup.

The spindle alignment method makes use of the in-built capability of modern NC controllers to specify the orientation of the spindle. The XYZ 1020 VMC machine tool used throughout the experiments possesses a Siemens 840D SL controller, which has the option to specify the orientation of the spindle via the following command:

$$SPOS = 120(\text{ orientate the spindle at 120 degrees})$$

Equivalent functionality is available on most modern NC controllers, such as the Fanuc 31i, which uses the M19 command for similar purposes. A schematic of a misaligned tool being rotated in the spindle is shown in Figure 8.

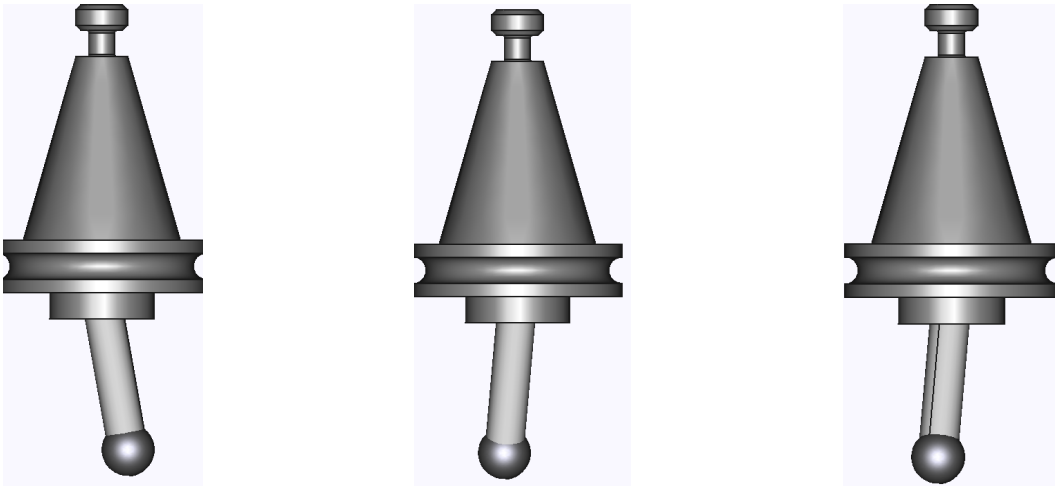

Figure 8: A misaligned tool-cup being rotated in the spindle of the machine tool

For tests that are sensitive to radial tool-cup errors (radial B-axis tests and radial C-axis tests), the spindle-indexing method works as follows. Assuming the absence of spindle tilt errors, a rotation of the spindle will change the direction of the radial tool-cup errors, but will not change their magnitude. The use of three uniformly distributed spindle orientations over a full 360° spindle rotation is sufficient to cancel the effects of radial tool-cup errors. This may be thought of as taking the arithmetic mean of the X and Y coordinates of three points on the perimeter of a circle, each separated by 120°. This analogy transfers to TMBB radially aligned TMBB tests, as running three radially aligned tests, back-to-back, at spindle orientations of 0, 120 and 240 will result in a similar cancellation.

Figure 9 shows the principle of the spindle indexing method working within the VMT. It can be seen that in radial B-axis tests, tool-cup set-up errors affect the identification of the radial offset errors in the X-direction, but not the Z-direction. These simulations are conducted with no other errors acting in the system and tool-cup errors are set to 10 and 20μm for the X and Y-directions, respectively. By taking the average of the centroids of the least squares circle for SPOS = 0°, 120° and 240°, these effects are duly cancelled, revealing no residual effect. The same can be said for the radial C-axis test; however, radial offsets in the X and Y-directions are both susceptible to corruption.

Figure 10 shows the detrimental effects of tool-cup errors in the Z-direction for the radial B-axis test. It can be seen that incorrectly measured tool-cup length will result in a falsification of the radial offset error in the Z-direction. This result has a one-to-one ratio, shown here as a 10μm tool-cup error resulting in a 10μm error in the identified radial offset error, which is set to zero in these tests (along with all other system errors).

Linear axis squareness errors have a variety of effects on the rotary axis tests. These are shown in Figure 11, where examples of isolated effects are given (i.e. all other errors are set to zero). Squareness error between the X and Y-axes (E_{C0X}) significantly affects both the axial B-axis and radial C-axis tests. In the axial B-axis tests, the Y-component in the X-axis gives the appearance of a rotary axis tilt error about the Z-direction. A similar effect can be seen for the Axial B-axis test in the presence of a squareness error between the Z and Y-axes (E_{A0Z}); this time giving the impression of a rotary axis tilt error about the X-direction. In the radial C-axis test, the linear axis squareness error results in a familiar elliptical appearance of the TMBB extension, which can affect least-squares circle fitting.

Squareness error between the Z and X-axes affects both radial B and radial C-axis tests. In the radial B-axis test, an elliptical appearance is seen, but this time with eccentricity. The elliptical appearance stems from the elliptical path resulting from the squareness error. The eccentricity is present because the Z-axis squareness error results in an incorrect positioning of the tool-tip in the Y-direction, changing the perpendicular separation of the tool-tip and nominal Z-axis. When a circular interpolation is conducted

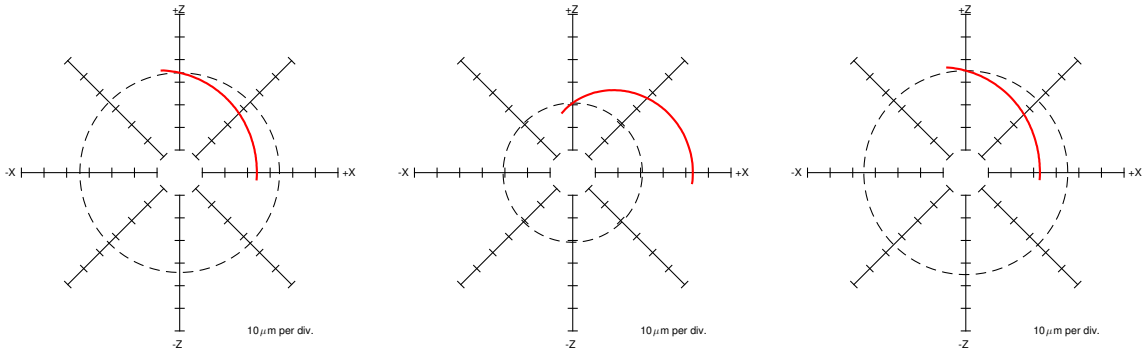

C_x [μm]	C_z [μm]	C_x [μm]	C_z [μm]	C_x [μm]	C_z [μm]
−10.0	0.0	22.3	0.0	−12.3	0.0

Mean C_x [μm]	Mean C_z [μm]
0.0	0.0

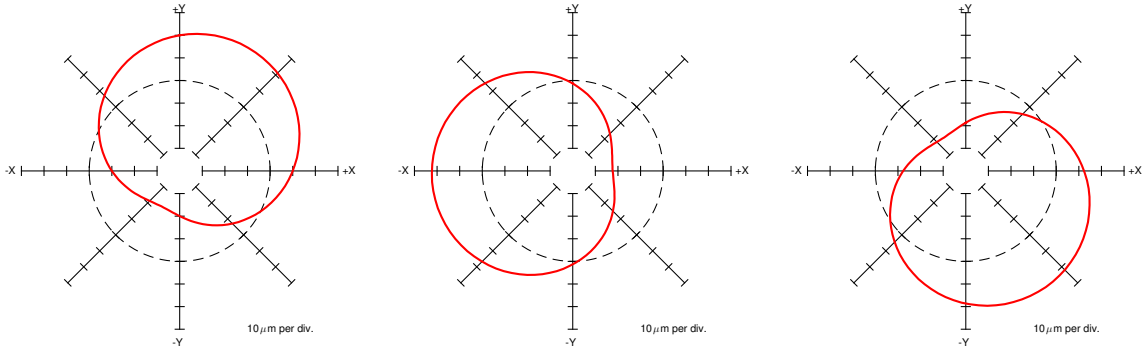

C_x [μm]	C_y [μm]	C_x [μm]	C_y [μm]	C_x [μm]	C_y [μm]
−10.0	−20.0	22.3	1.3	−12.3	18.7

Mean C_x [μm]	Mean C_y [μm]
0.0	0.0

Figure 9: Diagrams showing the spindle-indexing method applied to the radial B and radial C-axis tests using the VMT

by the tool-tip as it traces the centre-pivot motion, it gives the impression of an offset in the rotary axis average line in the X-direction. This eccentricity is also present in the radial C-axis test; however, the elliptical appearance is not present due to the interpolation being carried out in the XY-plane (with no Z-component). The same phenomenon is also clearly seen for the radial C-axis test when a squareness error exists between the Z and Y-axes, giving the B-axis the impression of a radial offset error in the Y-direction.

To demonstrate that the methods detailed in this research can accurately identify rotary axis location errors in the presence of set-up errors and linear axis squareness errors, the VMT is used. In this study, all location errors are populated with random values. Subsequently, all testing toolpaths are simulated and error diagnosis algorithms are used to predict the 'given' error values. It is assumed that the linear axis squareness errors have been accurately measured prior to rotary axis testing, using three planar TMBB tests.

For each rotary axis, a point on the rotary axis average line is identified and a direction unit vector describing the orientation of the axis is attached to this point. From this representation the rotary axes are expressed in accordance with the error definitions given in Table 1. The given and identified error values for this experiment are presented in Table 3.

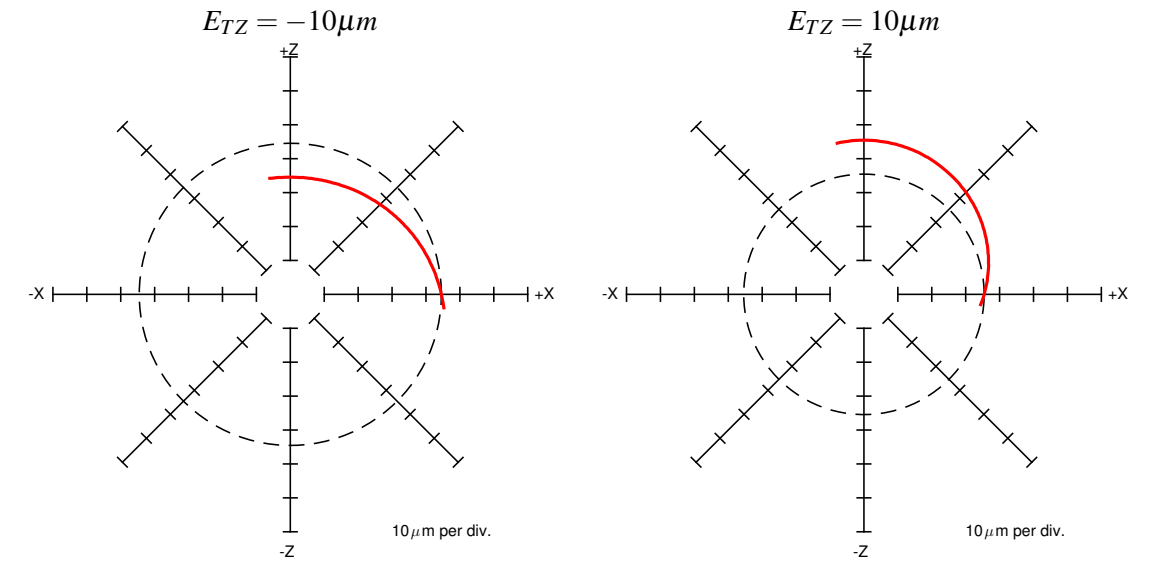

$C_x\ [\mu m]$	$C_z\ [\mu m]$	$C_x\ [\mu m]$	$C_z\ [\mu m]$
0.0	-10.0	0.0	10.0

Figure 10: Diagram showing the effects of tool-cup errors in the Z-direction of the radial B-axis test

Table 3: Error diagnosis results from experiments conducted within the VMT

Error		Given	Identified	Residual Error	% Identification Error
E_{C0X}	$[\mu m/m]$	32.5	-	-	-
E_{A0Z}	$[\mu m/m]$	-29.8	-	-	-
E_{B0Z}	$[\mu m/m]$	33.1	-	-	-
E_{XT}	$[\mu m]$	-20.0	-	-	-
E_{YT}	$[\mu m]$	-34.0	-	-	-
E_{ZT}	$[\mu m]$	5.0	-	-	-
E_{XW}	$[\mu m]$	-94.0	-	-	-
E_{YW}	$[\mu m]$	36.0	-	-	-
E_{ZW}	$[\mu m]$	-19.0	-	-	-
E_{AOB}	$[\mu m/m]$	-45.7	-44.9	0.8	-1.7
E_{C0B}	$[\mu m/m]$	62.7	62.2	-0.5	-0.8
E_{X0B}	$[\mu m]$	91.4	93.5	2.1	2.3
E_{A0C}	$[\mu m/m]$	85.7	83.4	-2.3	-2.7
E_{B0C}	$[\mu m/m]$	-47.7	-47.8	-0.1	-0.2

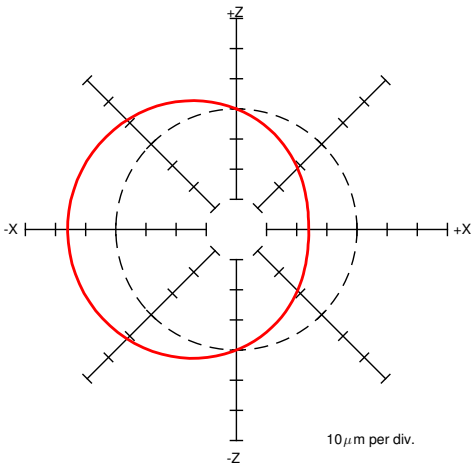

Axial B: $E_{C0X} = 100\mu m/m$

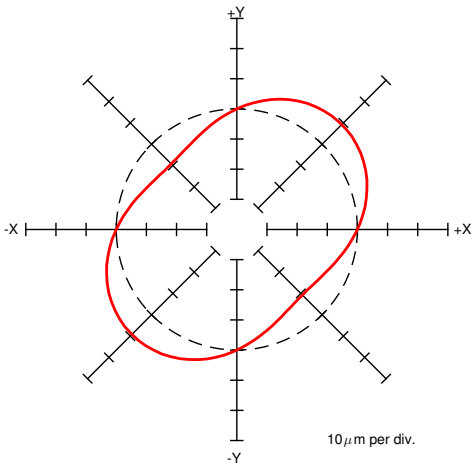

Radial C: $E_{C0X} = 100\mu m/m$

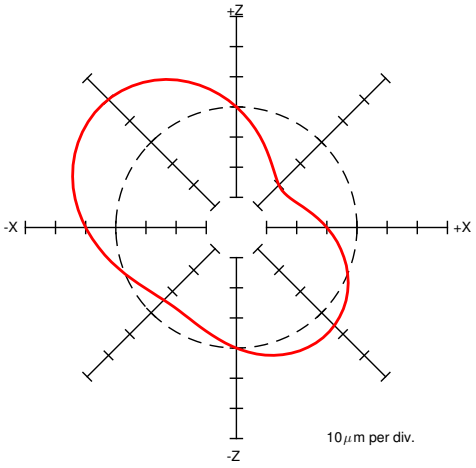

Radial B: $E_{B0Z} = 100\mu m/m$

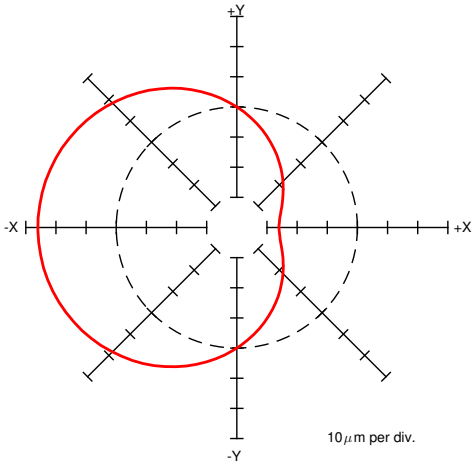

Radial C: $E_{B0Z} = 100\mu m/m$

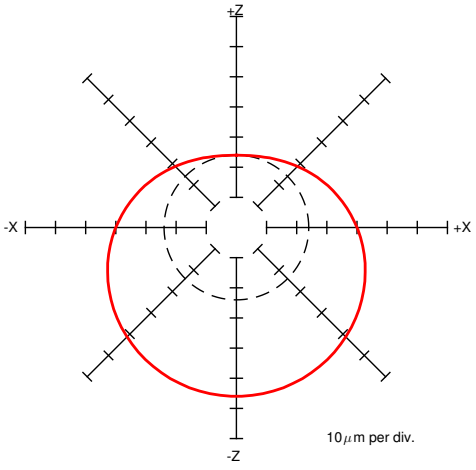

Axial B: $E_{A0Z} = 100\mu m/m$

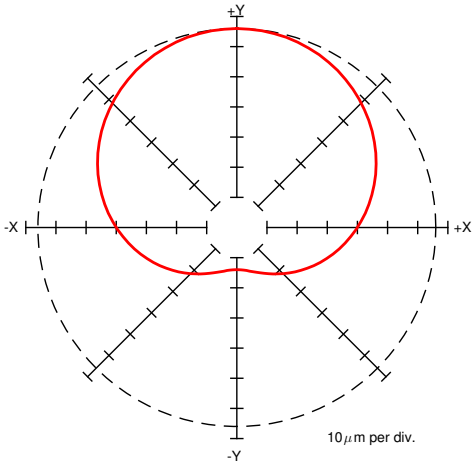

Radial C: $E_{A0Z} = 100\mu m/m$

Figure 11: Simulating the effects of linear axis squareness errors on rotary axis tests using the VMT

It can be seen from Table 3 that the testing procedure and error identification techniques proposed in this research can accurately identify all necessary location errors inherent to the rotary axes, whilst remaining robust in the presence of set-up and linear axis location error effects. The maximum percentage error in the identified parameters is 2.7%, highlighting the viability of the proposed method. It should be noted that the presence of tool-cup error in the Z-direction will have resulted in an incorrect specification of the machine tool origin's Z-coordinate, which is not made clear in these error definitions. In the present method, this effect can only be reduced through accurately measuring the tool-cup length.

3 Experimental verification

For each of the techniques outlined in the previous section, experiments have been designed to validate the individual methods and also the VMT model as a development platform. Focus is given to comparing the spindle-indexing method, linear axis squareness removal, and an assessment of the limitations and advantages of conducting all tests from a single testing set-up.

3.1 Suppression and compensation of set-up error effects

To demonstrate the efficacy of the spindle-indexing method outlined in Section 2.8, experiments were conducted to facilitate a comparative study of manual tool-cup alignment vs. spindle-indexing. Firstly, the radial B-axis and radial C-axis tests were conducted with a misaligned tool-cup and the spindle-indexing method (SPOS = 0, 120 and 240). The tool-cup was then aligned manually and the toolpaths were repeated using a single spindle orientation (SPOS = 0). The tool cup was deemed to be aligned if the change in TMBB length over a full spindle rotation was less than $3\mu m$. The identified radial coordinates of each rotary axis, identified via the least squares circle, were then compared.

For this experiment, a novel adjustable tool-cup was designed, which requires minimal separate and moving components. In addition to this, the device can be manufactured in a single installation within a turn-mill machine tool from widely available round-stock material, for ease of manufacture at a low cost-base. The principle of operation centres on the introduction of an intentional neck in the diameter of the device; visible in Figure 12 as the groove in the largest diameter of the tool-cup. Three M3 adjustment screws are travel axially through a tool-cup, pushing against a stationary face on one side of the aforementioned groove. By tightening and loosening these screws a small deflection is introduced in the necked section of the tool-cup, yielding a small lateral movement in the tool-tip. Employing this design permits minute adjustment of the tool-cup at the sub-micron level, making it ideal for realignment.

3.2 Suppression of linear axis location error effects

Firstly, the centre-pivot is mounted on the C-axis table, coincident with the C-axis average line as per the stored controller value. A conventional circular TMBB test is conducted in the XY-plane using a TMBB length of 100mm, in accordance with ISO 230-4:2005 [32].The squareness value was then taken from the Renishaw QC20 software [33] and was assumed to be the true value. Next, two radially aligned tests were conducted on the C-axis of the machine tool, as shown in Figure 13. In test 1, the tool-cup was placed on the perceived C-axis centre-line such that a radial C-axis test could be conducted without any linear axis motion. This represents the best possible case for suppression of linear axis squareness effects. In Test 2, the centre-pivot moves about the C-axis in a circle of radius 50mm, and the tool-cup moves in synchronisation in the XY-plane, following a circular path of 100mm. The principle objective behind this experiment was to identify the squareness errors between the X and Y-axis and then use this information to compensate the results gained from radial C-axis tests that use linear axis motion.

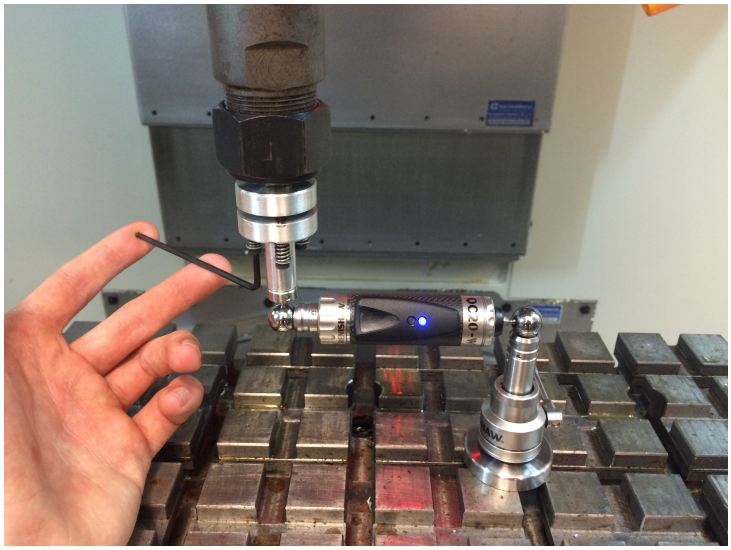

Figure 12: Alignment of the adjustable tool-cup, using the TMBB to check alignment during spindle rotation

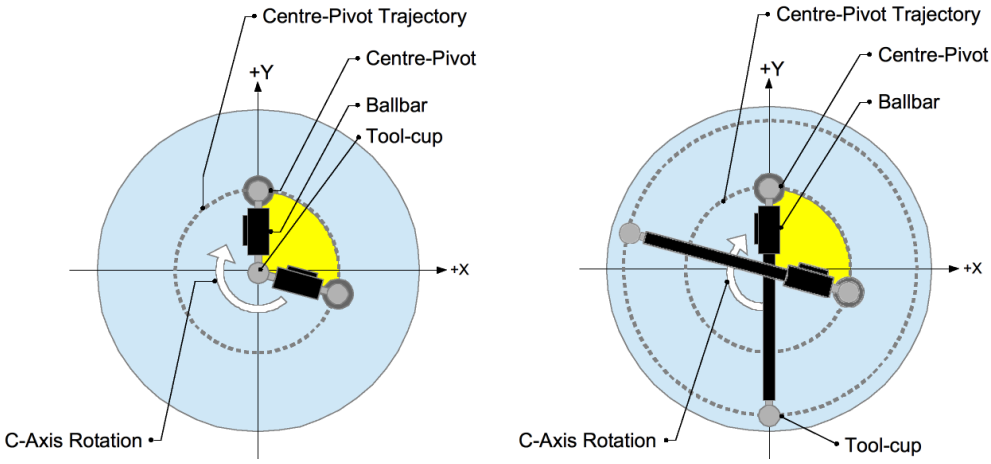

	Radial C: Test 1	Radial C: Test 2
L_0	50 mm	150 mm
CP_{start}	$[0mm, 50mm, 160mm]$	$[0mm, 50mm, 160mm]$
TC_{start}	$[0mm, 0mm, 160mm]$	$[0mm, -100mm, 160mm]$
C-axis	$0°, 115°$	$0°, 115°$

Figure 13: Experimental procedure and parameters to test the suppression of linear axis location errors during rotary axis

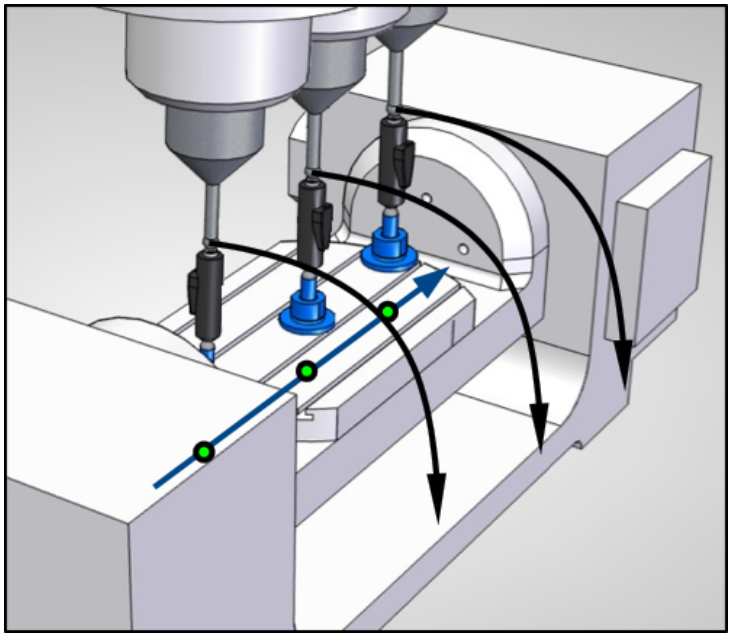

Figure 14: Three testing positions used to establish the efficacy of the single set-up method

3.3 Analysing the repeatability of the proposed method

To make an assessment of the repeatability of the combined methods proposed in this research, two sets of repeated measurements were conducted. Axial and radial tests for both rotary axes were conducted at two offset centre-pivot locations: $O_y = -85mm$ and $O_y = 85mm$. Additionally, the axial and radial B-axis tests, and three planar linear axis tests were conducted with the centre pivot a central location ($O_y = 0mm$). The three testing locations are depicted in Figure 14.

Two types of repeats were gathered for this investigation. The first type requires the centre-pivot and tool-cup to be installed once. Then, 31 repeats of the axial B, radial B, axial C and radial C toolpaths were conducted using the same centre-pivot and tool-cup set-up in the $O_y = -85mm$ centre-pivot position. This gave an indication of the repeatability of the machine tool and TMBB combination, without the influence of set-up-related uncertainty. In the second type, all four rotary axis toolpaths were conducted at the $O_y = 85mm$ and $O_y = -85mm$ centre-pivot positions. In addition to this, both B-axis toolpaths and the linear axis tests are conducted at the $O_y = 0mm$ position. To reduce the likelihood of time or temperature-dependent influences obscuring the results, a single repeat of the measurements was taken at each of the centre-pivot location, consecutively. When the centre-pivot was moved to a new location, the centre-pivot and tool-cup were reinstalled to provide a fresh set of set-up errors. All three centre-pivot locations were visited 15 times in total to provide repeated measurements.

The second type of repeats serves two purposes. Firstly, it gives an indication of the change in repeatability in the measured quantities, when a new set-up is used each time. For a procedure that is completely robust, there should be no significant change to the standard deviation in the measured rotary axis error parameters if a new set-up is used in each repeat. Secondly, errors measured at different centre-pivot location could be compared. The rotary axis error parameters identified using an offset centre-pivot location are transported back to the machine tool origin using the method described in Section 2.7. To allow conclusions to be drawn about effects of testing in an unconventional location, the error values were compared to those taken with the centre-pivot in the central location ($O_y = 0mm$), which are assumed to be the true values.

4 Analysis and discussion

The experimental data captured using the experiments defined in the previous section has been analysed to identify the strength and limitations of the proposed techniques. In particular, attention is given to the ability to remove set-up and linear axis squareness error effects. This then leads into a statistical assessment of the agreement between errors identified at different centre-pivot locations.

4.1 Suppression and compensation of set-up error effects

Having conducted the experiments outlines in Section 3, the identified radial coordinates of the rotary axis average line were compared for the manually-aligned tool-cup method and the spindle indexing method. A statistical t-Test was conducted for each radial coordinate and the calculated probability, p-values are reported in Table 4. A total of five sample measurements were used in this analysis, with 95% confidence.

For radial *B*-axis testing, there was no significant difference between the means for both *X* and *Z* directions, indicating there is not enough evidence to suggest that there is a difference between the two methods. In radial *C*-axis testing, there is a significant difference between the Spindle indexing method and manual tool alignment method; however, the difference between the means is less than $2\mu m$. A tool was assumed to be aligned if a deviation of $3\mu m$ (or less) was present, justifying this difference.

4.2 Removal of linear axis location error effects

Tests were conducted in accordance with Section 3.2 to identify whether the proposed compensation scheme to remove linear axis location error effects from rotary axis test was successful. The spindle indexing method has been used in all tool-paths for this investigation. The means of the tests with no tool motion (Test 1), tests with tool motion but no compensation (Test 2) and tests using tool motion and compensation (Test 3) where compared using a t-Test and p-values were calculated. The values from Test 1 were taken as the actual values, allowing residuals to be calculated for the other two tests. Each radial coordinate was considered in isolation and the results are reported in Table 5 for a total of 11 repeated measurements. Additionally, interval plots are shown for the radial coordinates of the *C*-axis average line identified in each of the three tests in Figure 15.

The analysis indicated that there is a difference between the three methods. Analysis of the means revealed that the uncompensated residuals deviate from the no-tool-motion method by -10%, -27% for *X* and *Y* radial coordinates, respectively. Compensated residuals only deviate by 3% and 1%, highlighting the viability of the proposed compensation for minimising the deviation. Finally, experimental data is used to identify the how the set-up procedure affects the repeatability of the measurement outcomes.

4.3 Transporting and expressing error values at the machine tool origin

The first point of discussion is the need for the unit vector components of the *B*-axis to be the same, regardless of the centre-pivot position during the axial *B*-axis tests. Statistical comparison of the mean val-

Table 4: Statistical measures comparing the means of tests conducted with an aligned tool-cup (Align) and the spindle-indexing method (S.I.)

	B-Axis				*C*-Axis			
	C_x		C_z		C_x		C_y	
	Align	S.I.	Align	S.I.	Align	S.I.	Align	S.I.
Mean $[\mu m]$	-60.7	-61.7	-13.6	-12.5	-27.0	-25.4	-9.1	-8.6
p-value	$\leftarrow 0.291 \rightarrow$		$\leftarrow 0.682 \rightarrow$		$\leftarrow 0.006 \rightarrow$		$\leftarrow 0.701 \rightarrow$	

Table 5: Statistical measures relating to the removal linear axis squareness error effects

	C_x			C_y		
	Test 1	Test 2	Test 3	Test 1	Test 2	Test 3
Mean $[\mu m]$	-24.9	-22.4	-25.6	-11.6	-8.5	-11.7
Mean Residual $[\mu m]$	0.0	2.6	-0.7	0.0	3.1	-0.1
p-value: Test 1 vs. Test 2		1.23×10^{-9}			3.08×10^{-5}	
p-value: Test 2 vs. Test 3		6.88×10^{-4}			8.60×10^{-1}	

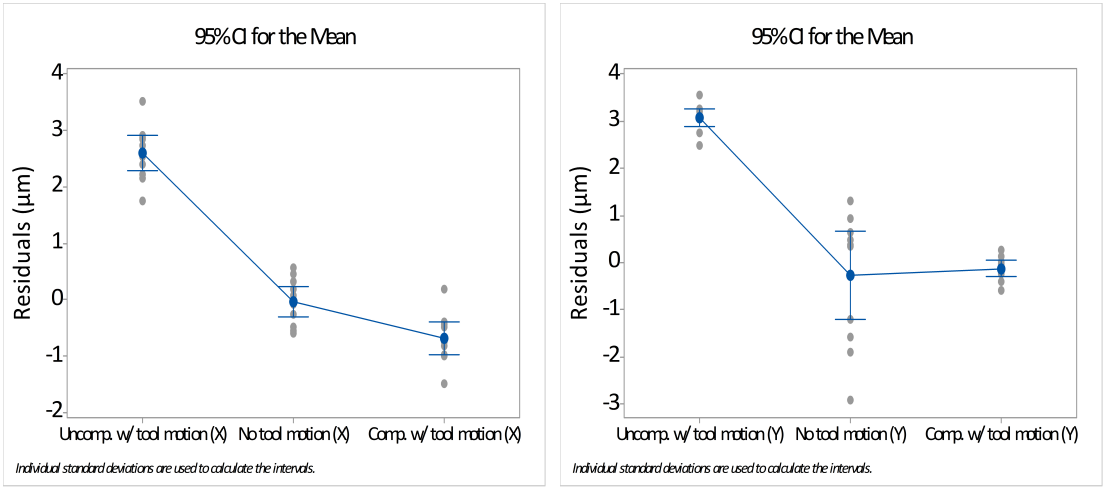

(a) (b)

Figure 15: Interval plots comparing the effects of linear axis location error compensation on the identification of the X (a) and Y (b) radial coordinates of the C-axis average line

ues indicated that there was a significant difference between testing locations (negative, centre and positive) for B-axis tests. However, the percentage difference between the means were 4% (X-component) and -15% (Z-component) in the negative testing location, and -5% (X-component) and 21% (Z-component) for the positive testing location. Conducting a similar analysis for the axial C-axis test showed that there was insufficient evidence to reject the null hypothesis that the means were equal. Similar testing results can be expected from either the positive or negative location.

On a machine tool of this size (C-Table diameter = 200mm), these differences in the B-axis readings result in radial coordinate deviations in the average line of $0.374\mu m$ (X-direction), $1.01\mu m$ (Z-direction) at the negative location and $1.25\mu m$ (X-direction) and $4.40\mu m$ (Z-direction) at the positive location. These are sufficiently low for all values to be considered for compensation. The mismatch between the data casts doubt on the assumption that location errors are sufficient to characterise a machine tool's kinematic behaviour. It also highlights the need to specify the location at which a test was conducted. It is suggested that a rotary axis that is mounted upon a linear axis may have its orientation changed by angular component errors in linear axes (in this case Y). This would explain the discrepancies between the three data sets.

The second requirement to support the notion of using offset testing location for the B-axis is that the radial coordinates of the B-axis average line are increasing or decreasing monotonically. More specifically, the radial coordinates should be connected by a straight line (the axis average line) in an ideal case. Inspection of Figure 16 shows that the values are increasing monotonically; however, they do not lie on a perfect straight line. This is attributed to the presence of component errors in Y-axis,

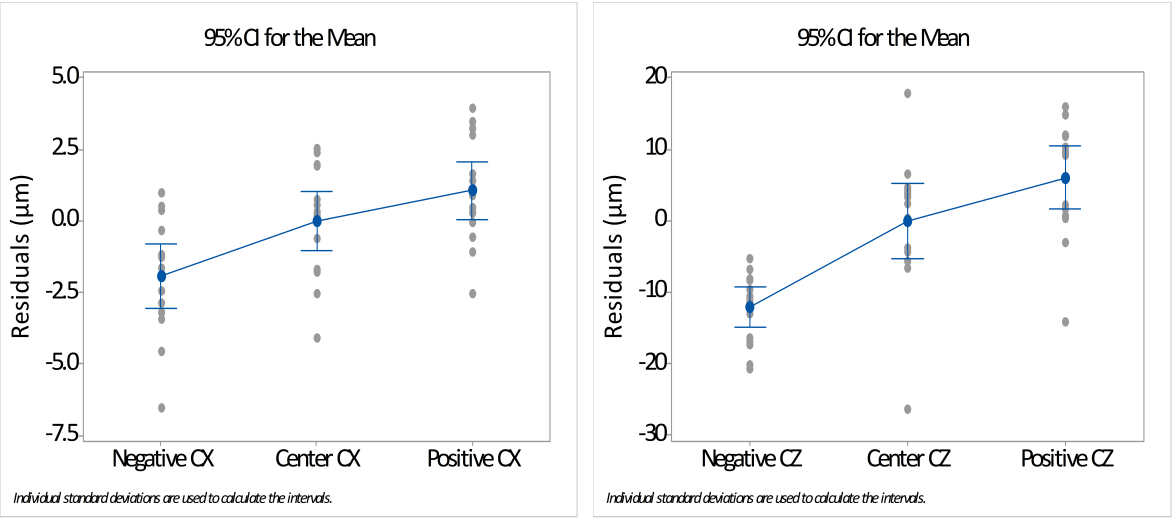

(a) (b)

Figure 16: Residuals of identified radial coordinates of the B-axis, compared against the true values measured with $O_y = 0mm$, showing values increasing monotonically, as predicted

minutely changing the position of the B-axis average line between centre-pivot locations.

To successfully transport error values for the B-axis, measured in an offset location ($O_y = \pm 85mm$), the point on the average line and the direction unit vector of the average line must be correctly identified. It is proposed that the methods outlined to deal with set-up errors and the linear axis location error effects will facilitate accurate prediction. To show that this has been achieved, the axis error parameters identified without any compensation are used project the offset readings to the centre position. They are then compared against the values that were actually measured in the centre position to assess the agreement between the two sets of values. Figure 17a and Figure 18a show the residuals between the projected values and measured values at the centre position ($O_y = 0mm$). Following this, the error parameters identified using the linear axis location error compensation technique are projected and compared with the values measured at the central position. These results are shown in Figure 17b and Figure 18b.

The mean residual errors for values without compensation are $5.5\mu m$ and $3.7\mu m$ for C_x and C_z in negative centre-pivot position, respectively. For the positive centre-pivot position, the residual are $-7.5\mu m$ and $-12.2\mu m$, respectively. The compensated values are $1.9\mu m$ and $-2.8\mu m$, and $-2.1\mu m$ and $-4.5\mu m$. Comparing the mean residual errors in the projected error parameters, it can be seen that values with linear squareness removal give an improved prediction in all cases, highlighting the viability of the proposed methodology. It should be noted that none of the linear axis squareness errors exceeded $50\mu m/m$. Machines with more severe linear axis squareness errors would benefit to an even greater extent from the compensation proposed in this research.

4.4 Analysing the repeatability of the proposed method

When each repeated measurement uses a new installation of the centre-pivot and tool-cup ('Multi' in Table 6), a larger standard deviation is observed in each error parameter when compared to readings with only one centre-pivot and tool-cup installation ('B2B' in Table 6). This can be explained by the fact that new set-up errors are introduced by each set-up procedure, affecting the analysis. Considering this, all error parameters outlined in this research include these deviations, which places them within an acceptable range for machine tool verification and compensation purposes.

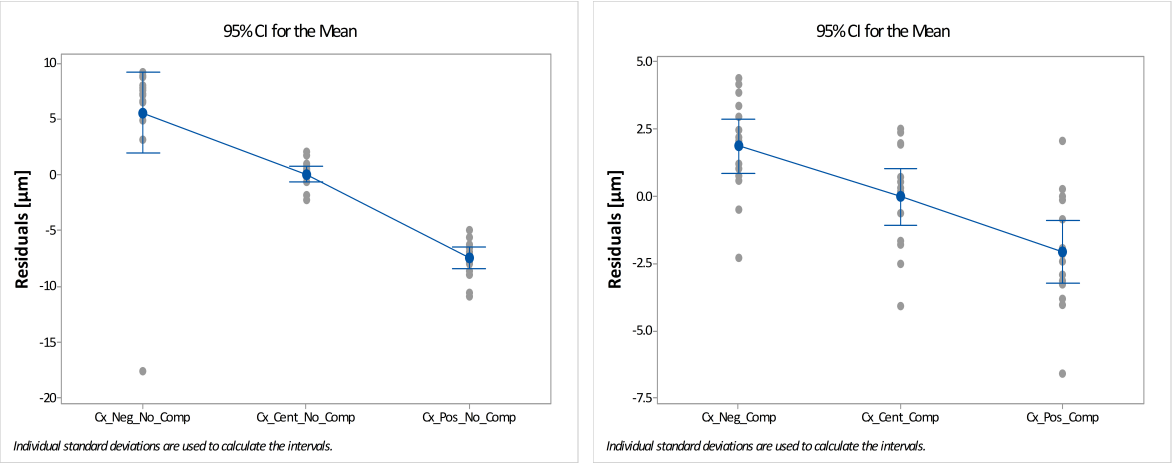

(a) (b)

Figure 17: Error residuals resulting from projecting B-axis radial offset error in X-direction back to the central position ($O_y = 0mm$) for (a) values without linear location error compensation, and (b) error values with linear location error compensation

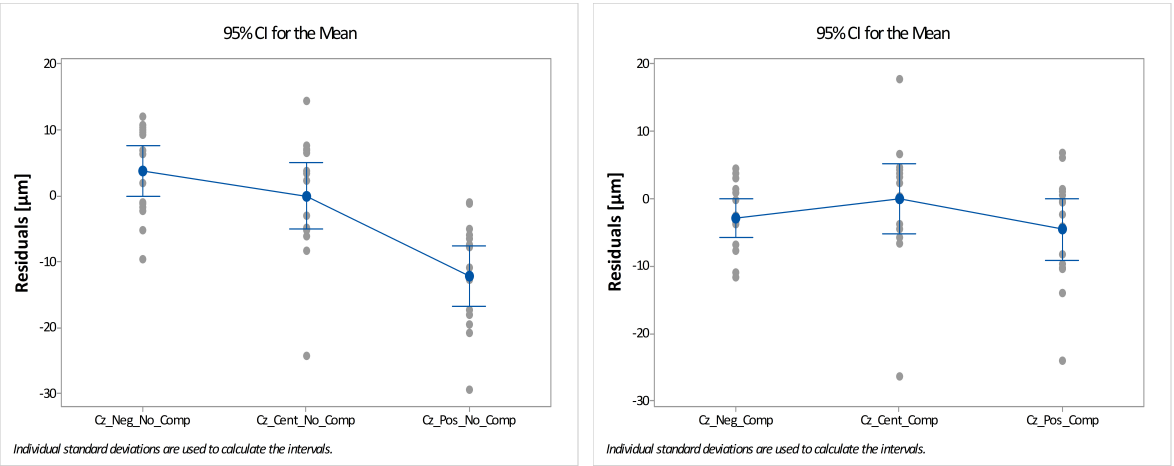

(a) (b)

Figure 18: Error residuals resulting from projecting B-axis radial offset error in Z-direction back to the central position ($O_y = 0mm$) for (a) values without linear location error compensation, and (b) error values with linear location error compensation

Table 6: Statistical measures relating to the removal linear axis squareness error effects

	Radial-B		Axial-B		Radial-C		Axial-C	
	C_x $[\mu m]$	C_z $[\mu m]$	U_x $[\mu m/m]$	U_z $[\mu m/m]$	C_x $[\mu m]$	C_y $[\mu m]$	U_x $[\mu m/m]$	U_y $[\mu m/m]$
Std. dev.: B2B	0.41	1.32	1.28	1.18	0.09	0.24	0.85	1.48
Std. dev.: Multi	2.02	5.16	4.03	9.08	1.22	2.58	4.46	6.62

5 Conclusions and future research

The virtual machine tool presented in this paper creates an environment for the design and testing of new ballbar testing methods for 5-axis machine tools. This led to the design of a single set-up testing method to identify all location errors inherent to a 5-axis machine tool. The method allows the measurement process to be highly-automated and removes the need for modified hardware to remove set-up errors. It is also robust in the presence of linear axis squareness effects, increasing the usefulness and trustworthiness of the measured data. This has only been achieved previously using kinematic model-based optimisation to fit machine tool errors to TMBB measurements. Errors measured in the single-set-up location were able to predict the errors measured in conventional locations with mean prediction errors below $4.5\mu m$, validating the rotary axis average line characterisation. The new set-up procedure for the TMBB apparatus does not significantly degrade the repeatability of the error identification process. The maximum increases in standard deviation were $3.8\mu m$ and $7.9\mu m/m$ for offset and tilt-errors, respectively, which shows the robustness to set-up errors. This new testing method relates closely to standardised testing methods, adding no additional complication. It can be used in place of multi-set-up methods to reduce machine tool down-time, and the need for high-levels of operator skill and dexterity. By reducing testing durations and stringent set-up requirements, this research will impact 5-axis machine tool users by encouraging them to frequently verify the kinematic errors within their machines, giving an accurate and up-to-date representation of their machining capability. Future research will consider Monte Carlo uncertainty analysis of the new method and will also explore the transformation of identified error values into controller compensation parameters. Finally, further exploration of including multiple three-axis TMBB tests, using the will form part of the future research.

Acknowledgements

The authors are pleased to thank the Engineering and Physical Science Research Council (EPSRC No. EP/K504245/1) and our industrial partner for their support during this research.

References

[1] P A McKeown. The Role of Precision Engineering in Manufacturing of the Future. *CIRP Annals - Manufacturing Technology*, 36(2):495–501, 1987.

[2] H. Schwenke, W. Knapp, H. Haitjema, A. Weckenmann, R. Schmitt, and F. Delbressine. Geometric error measurement and compensation of machinesAn update. *CIRP Annals - Manufacturing Technology*, 57(2):660–675, jan 2008.

[3] Soichi Ibaraki and Wolfgang Knapp. Indirect Measurement of Volumetric Accuracy for Three-Axis and Five-Axis Machine Tools : A Review. *International Journal of Automation Technology*, 6(2):110–124, 2012.

[4] J B Bryan. A simple method for testing measuring machines and machine tools. *Precision Engineering*, 4(2):61–69, 1982.

[5] ISO. ISO 230-1:2012: Test code for machine tools – Part 1: Geometric accuracy of machines operating under no-load or quasi-static conditions, 2012.

[6] ISO. ISO 10791-6:2014: Test conditions for machining centres – Part 6: Accuracy of sppeds and interpolations, 2014.

[7] Y Kakino, Y Ihara, K Satou, and H Ohtubo. A Study on the motion accuracy of NC machine tools (7th report): the measurement of motion accuracy of 5 axis machine by DBB test. *Journal of the Japan Society for Precision Engineering*, 60(5):718–722, 1994.

[8] S Sakamoto and I Inasaki. Identification of Alignment Errors in Five-Axis Machining Centers. *Transaction of Japan Society for Mechanical Engineers*, 60(575), 1994.

[9] M. Tsutsumi and a. Saito. Identification and compensation of systematic deviations particular to 5-axis machining centers. *International Journal of Machine Tools and Manufacture*, 43(8):771–780, jun 2003.

[10] Masaomi Tsutsumi, Shintaro Tone, Noriyuki Kato, and Ryuta Sato. Enhancement of geometric accuracy of five-axis machining centers based on identification and compensation of geometric deviations. *International Journal of Machine Tools and Manufacture*, 68:11–20, may 2013.

[11] S.H.H. Zargarbashi and J.R.R. Mayer. Assessment of machine tool trunnion axis motion error, using magnetic double ball bar. *International Journal of Machine Tools and Manufacture*, 46(14): 1823–1834, nov 2006.

[12] Kwang-il Lee, Dong-mok Lee, and Seung-han Yang. Parametric modeling and estimation of geometric errors for a rotary axis using double ball-bar. *Internation Journal of Advanced Manufacturing Technology*, 62:741–750, 2012.

[13] Sitong Xiang, Jianguo Yang, and Yi Zhang. Using a double ball bar to identify position-independent geometric errors on the rotary axes of five-axis machine tools. *The International Journal of Advanced Manufacturing Technology*, 70(9-12):2071–2082, 2014.

[14] Kwang-Il Lee and Seung-Han Yang. Compensation of position-independent and position-dependent geometric errors in the rotary axes of five-axis machine tools with a tilting rotary table. *The International Journal of Advanced Manufacturing Technology*, 2015.

[15] S. H. H. Zargarbashi and J. Angeles. Identification of error sources in a five-axis machine tool using FFT analysis. *The International Journal of Advanced Manufacturing Technology*, 76(5-8): 1353–1363, 2015.

[16] Kwang Il Lee and Seung Han Yang. Robust measurement method and uncertainty analysis for position-independent geometric errors of a rotary axis using a double ball-bar. *International Journal of Precision Engineering and Manufacturing*, 14(2):231–239, 2013.

[17] Xiaogeng Jiang and Robert J. Cripps. A method of testing position independent geometric errors in rotary axes of a five-axis machine tool using a double ball bar. *International Journal of Machine Tools and Manufacture*, 89:151–158, feb 2015.

[18] Abdul Wahid Khan and Wuyi Chen. A methodology for error characterization and quantification in rotary joints of multi-axis machine tools. *International Journal of Advanced Manufacturing Technology*, 51(9-12):1009–1022, 2010.

[19] Yi Zhang, Jianguo Yang, and Kun Zhang. Geometric error measurement and compensation for the rotary table of five-axis machine tool with double ballbar. *International Journal of Advanced Manufacturing Technology*, 65(1-4):275–281, 2013.

[20] Min Wang, Jianzhong Hu, and Tao Zan. Kinematic error separation on five-axis NC machine tool based on telescoping double ball bar. *Frontiers of Mechanical Engineering in China*, 5(4): 431–437, sep 2010.

[21] Y Abbaszadeh-Mir, J R R Mayer, G Cloutier, and C Fortin. Theory and simulation for the identification of the link geometric errors for a five- axis machine tool using a telescoping magnetic ball-bar. *Internation Journal of Production Research*, 40(18):4781–4797, 2002.

[22] Jixiang Yang, J.R.R. Mayer, and Yusuf Altintas. A Position Independent Geometric Errors Identification and Correction Method for FiveAxis Serial Machines based on Screw Theory. *International Journal of Machine Tools and Manufacture*, 95:52–66, 2015.

[23] Zhimeng Li, Masaomi Tsutsumi, and Noriyuki Kato. Identification and compensation of geometric deviations including squareness of translational axes in five-axis machining centers. In *Proceedings of the Japanese Society of Precision Engineering Annual Spring Conference [in Japanese]*, number 2, pages 701–702, 2013.

[24] Masaomi Tsutsumi, Naoki Miyama, Shintaro Tone, Akinori Saito, Chengri Cui, and K M Muditha Dasssanayake. Correction of Squareness of Translational Axes for Identification of Geometric Deviations Inherent to Five-Axis Machining Centres with a Tilting-Rotary Table. *Japan Society of Mechanical Engineers (Series C) [in Japanese]*, 79(799), 2013.

[25] Kwang-Il Lee and Seung-Han Yang. Measurement and verification of position-independent geometric errors of a five-axis machine tool using a double ball-bar. *International Journal of Machine Tools and Manufacture*, 70:45–52, jul 2013.

[26] Masaomi Tsutsumi and Akinori Saito. Identification of angular and positional deviations inherent to 5-axis machining centers with a tilting-rotary table by simultaneous four-axis control movements. *International Journal of Machine Tools and Manufacture*, 44(12-13):1333–1342, oct 2004.

[27] ISO. ISO 841:2001: Industrial Automation Systems and Integration - Numerical Control of Machines - Coordinate System and Motion Nomenclature, 2001.

[28] Ronnie R. Fesperman, Shawn P. Moylan, Gregory W. Vogl, and M. Alkan Donmez. Reconfigurable data driven virtual machine tool: Geometric error modeling and evaluation. *CIRP Journal of Manufacturing Science and Technology*, 10:120–130, 2015.

[29] MathWorks, Inc. MATLAB R2014b, 2014.

[30] Ali Al-Sharadqah and Nikolai Chernov. Error analysis for circle fitting algorithms. *Electronic Journal of Statistics*, 3:886–911, 2009.

[31] C.M. Shakarji. Least-squares fitting algorithms of the NIST algorithm testing system. *Journal of Research of the National Institute of Standards and Technology*, 103(6):633, 1998.

[32] ISO. ISO 230-4:2005: Test code for machine tools – Part 4: Circular tests for numerically controlled machine tools, 2005.

[33] Renishaw. QC20-W ballbar system, 2013. URL `http://www.renishaw.com/en/qc20-w-ballbar-system--11075`.